Atmospheric Research 178–179 (2016) 304–319

Contents lists available at ScienceDirect

Atmospheric Research

journal homepage: www.elsevier.com/locate/atmosres

Lightning climatology in the Congo Basin

S. Soula [a,*], J. Kigotsi Kasereka [a,b], J.F. Georgis [a], C. Barthe [c]

[a] Laboratoire d'Aérologie, Université de Toulouse, CNRS, Toulouse, France
[b] Département de Physique, Faculté des Sciences, Université de Kinshasa, The Democratic Republic of the Congo
[c] LACy, UMR 8105, Météo-France/CNRS/Université de La Réunion, Saint-Denis, France

ARTICLE INFO

Article history:
Received 16 February 2016
Received in revised form 22 March 2016
Accepted 6 April 2016
Available online 13 April 2016

Keywords:
Lightning
Detection efficiency
Lightning density
Congo Basin

ABSTRACT

The lightning climatology of the Congo Basin including several countries of Central Africa is analysed in detail for the first time. It is based on data from the World Wide Lightning Location Network (WWLLN), for the period from 2005 to 2013. A comparison of these data with Lightning Imaging Sensor (LIS) data for the same period shows the relative detection efficiency of the WWLLN (DE) in the 2500 km × 2500 km region increases from about 1.70% in the beginning of the period to 5.90% in 2013, and it is in agreement with previous results for other regions of the world. However, the increase of DE is not uniform over the whole region. The average monthly flash rate describes an annual cycle with a strong activity from October to March and a low one from June to August, associated with the ITCZ migration but not exactly symmetrical on both sides of the equator. The zonal distribution of the lightning flashes exhibits a maximum between 1°S and 2°S and about 56% of the flashes are located south of the equator in the 10°S–10°N interval. The diurnal evolution of the flash rate has a maximum between 1400 and 1700 UTC, according to the reference year. The annual flash density and number of stormy days show a sharp maximum localized in the eastern part of Democratic Republic of Congo (DRC) regardless of the reference year and the period of the year. These maxima reach 12.86 fl km^{-2} and 189 days, respectively, in 2013, and correspond to a very active region located at the rear of the Virunga mountain range at altitudes that exceed 3000 m. The presence of these mountains plays a role in the thunderstorm development along the year. The estimation of this local maximum of the lightning density by taking into account the DE, leads to a value consistent with that of the global climatology by Christian et al. (2003).

1. Introduction

Space observations have shown that the highest concentrations of lightning on the Earth are mostly in the territory of the Democratic Republic of Congo (DRC). The global climatology of lightning activity developed by Christian et al. (2003) and based on data recorded during five years (May 1995–March 2000) by the Optical Transient Detector (OTD) loaded on board the satellite MicroLab-1, highlights the features of the lightning distribution on the globe and shows that the greatest rates of flashes are larger than 50 fl km^{-2} yr^{-1} and up to 82.7 fl km^{-2} yr^{-1} at a resolution of 0.25° × 0.25°, and they concern the equatorial region of the Congo Basin.

The Lightning Imaging Sensor (LIS) on board the Tropical Rainfall Measuring Mission (TRMM) satellite has detected lightning flashes for seventeen years (1997–2014). It provided a lightning climatology in a restricted area of the Earth between 38°S and 38°N. From three years observations (1998–2000), Williams and Stanfill (2002) analysed the land–ocean contrast of the lightning activity. As Christian et al. (2003) they concluded the maximum lightning activity is located in Central Africa. More recently, Cecil et al. (2014) detailed the characteristics of the lightning activity across the world from the combined data of LIS and OTD and confirmed the largest rate of lightning are observed in Central Africa. The peak of the annual flash rate was found in the East of the DRC with a value of 160 fl km^{-2} yr^{-1}.

Collier et al. (2006) developed a study of lightning activity from LIS data to establish statistical and seasonal distribution of the lightning activity in southern Africa. As in Christian et al. (2003), the highest density of lightning (107 fl km^{-2} yr^{-1}) was found in the Congo Basin. High lightning densities of 32.1 fl km^{-2} yr^{-1} and 26.4 fl km^{-2} yr^{-1} were also observed in Madagascar and South Africa, respectively, essentially during the austral summer. However, 13 years of LIS data have allowed to show that the local highest rate of lightning on the planet with 250 fl km^{-2} yr^{-1} is over the Lake Maracaibo in Zulia state in Venezuela, followed by the Congo Basin with 232 fl km^{-2} yr^{-1} (Albrecht et al., 2011). A more detailed study using LIS and World Wide Lightning Location Network (WWLLN) data has confirmed this strong local activity that exhibits two maxima related to the complex topography and specific climatic conditions (Burgesser et al., 2012). A more recent study analyzes in detail the lightning activity in northwestern Venezuela and highlights several factors at the origin of the

* Corresponding author at: Laboratoire d'Aérologie, 14 avenue Edouard Belin, 31400 Toulouse, France.
E-mail address: serge.soula@aero.obs-mip.fr (S. Soula).

http://dx.doi.org/10.1016/j.atmosres.2016.04.006
0169-8095/

Maracaibo maximum from LIS/OTD data, including large scale meteorological parameters and local drivers like convection triggered by the topographic configuration and the effect of the Maracaibo Basin Nocturnal Low Level Jet (Munoz et al., 2016).

The study by Christian et al. (2003) highlighted the relationship between lightning in the Congo Basin and the migration of the Intertropical Convergence Zone (ITCZ). An earlier study by Ba and Nicholson (1998) found that convection in the Congo Basin follows the migration of ITCZ. The airflow in the ITCZ latitudes band transports moisture from the Gulf of Guinea in the Congo Basin, that convection raises and leads to the formation of thunderclouds (Collier and Hughes, 2011). Several studies using data from regional and national ground-based networks of lightning detection, revealed how environmental parameters as the relief may affect the distribution of lightning (e.g. Hodanish et al., 1997; Soriano et al., 2005; Antonescu and Burcea, 2010).

Since the Congo Basin is the area where the number of lightning flashes is the largest on the planet, the forecast of thunderstorm activity is of great importance for the countries concerned. The detailed analysis of climatology of lightning activity proposed in this study aims to improve the knowledge of the frequency of storms in the region of Congo Basin, in terms of formation, location, time of occurrence, displacement and life time. It is also important to establish links between lightning and other violent phenomena associated with thunderstorms such as convective rains and violent winds, with a view to improve the immediate or very short-term storms forecasting and better prevent the risks of thunder-striking and violent phenomena associated with thunderstorms. The future lightning spatial detection planned with the satellite Meteosat Third Generation (MTG) will allow storms monitoring which enhances the interest to assess the relationship between lightning and other events such as heavy rain, violent wind and hail.

The main objective of this paper is to present for the first time in detail a study of the climatology of the lightning activity in the Congo Basin. The study area is geographically defined by 15°S–10°N in latitude and 10°E–35°E in longitude, in order to cover the whole Congo Basin and is indicated in Fig. 1 with a red square. This study is based on WWLLN data for the period from 2005 to 2013 that will be used to characterize the lightning activity in the Congo Basin. By using LIS data as a reference, we can assess the relative detection efficiency of the WWLLN network in the study area. In Section 2 we describe the data and in Section 3 we present the results in different sub-sections relative to time and space variability. Section 4 is devoted to discussion and summary.

2. Data

2.1. WWLLN data

Data from WWLLN recorded during nine years (2005 to 2013) have been used in order to study the temporal evolution of the lightning activity and its geographical distribution over a large area including and surrounding DRC territory. The WWLLN (www.wwlln.net/) is a global lightning detection network around the Earth. A Management Team, led by Prof Robert Holzworth of the University of Washington, collects these data with the cooperation of the universities and institutes which host the stations of detection. The electromagnetic radiations emitted by lightning strokes at very low frequency (VLF) and called sferics are detected by the sensors of the WWLLN. These strokes are then localized by using the time of group arrival technique (TOGA) (Dowden et al., 2002). The stations can be separated by thousands of km because the VLF frequencies can propagate within the Earth-Ionosphere wave guide with very little attenuation. The goal was to have about 60 sensors spaced uniformly about 3000 km apart to cover the whole world and to localize at least 50% of the CG flashes with an average accuracy better than 10 km (Rodger et al., 2005).

Since its implantation in March 2003, the WWLLN has been improved in terms of number of stations and development of the processing algorithm (Rodger et al., 2008). In 2014, it had more than 60 sensors spread on the planet (Fig. 1). Several authors have estimated

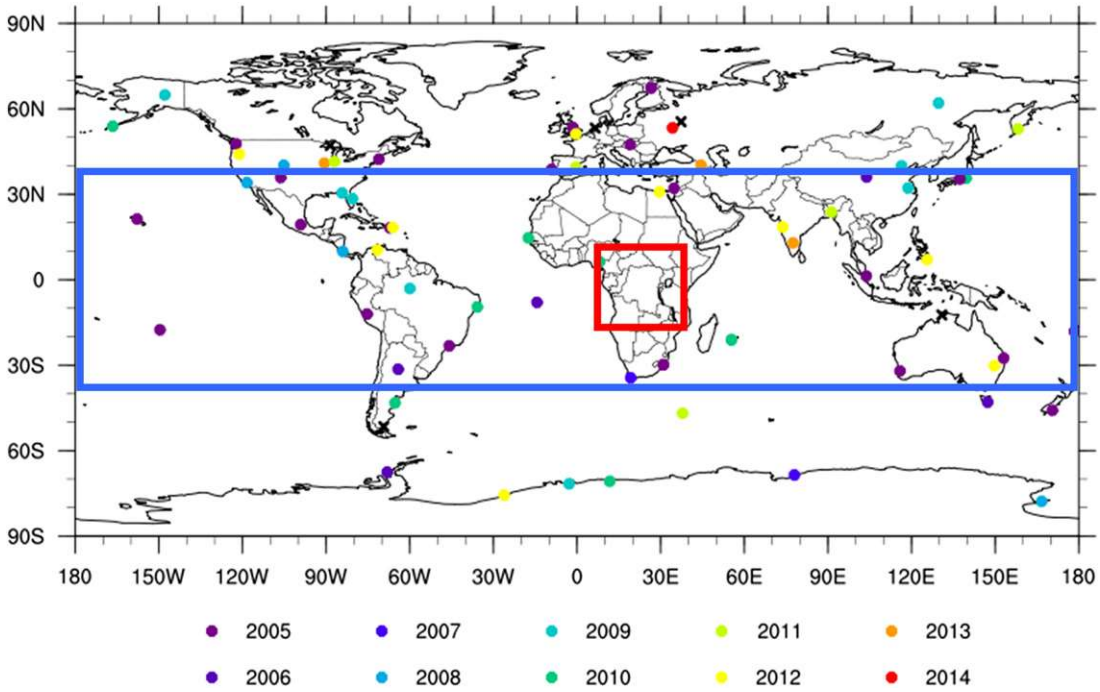

Fig. 1. Map of the WWLLN stations around the world. The colour provides the installation year as indicated in the legend. The red rectangle displays the study area (15°S–10°N; 10°E–35°E) and the blue rectangle the latitude band covered by LIS (38°S–38°N).

the evolution of DE for limited world regions and time periods by referring either to satellite data or to data provided from regional, national, or commercial flash detection networks (Rodger et al., 2005;. Rodger et al., 2006; Jacobson et al., 2006; Abarca et al., 2010; Abreu et al., 2010; Abarca and Corbosiero, 2011; DeMaria et al., 2012; Bovalo et al., 2012). Rodger et al. (2008) noted a large increase of stroke detections with additional sensors from 2003 to 2007: 10.6 million in March–December 2003 with 11 sensors to 28.1 million for the same period in 2007 with 30 sensors. Furthermore, they noted the improvements in the algorithm used to reconstruct the flashes from the WWLLN detections, increased DE for the network by 63% when it is applied on 2007 data. The WWLLN is capable of detecting both CG and IC lightning strokes with a comparable efficiency as long as their peak currents are comparable (Rodger et al., 2005, 2006; Jacobson et al., 2006). However, since CG strokes have higher peak currents, DE is about twice that of the IC strokes as reported by Bovalo et al. (2012). Recent research indicates that DE of the network is approximately 10% (35%) for strokes with a peak current larger than ±35 kA (−130 kA) (Abarca et al., 2010).

The WWLLN data have been used in various studies in the world as lightning climatology (Bovalo et al., 2012), convective activity in tropical cyclones (Abarca and Corbosiero, 2011; DeMaria et al., 2012; Bovalo et al., 2014), lightning activity for a thunderstorm producing gigantic jets at la Réunion Island (Soula et al., 2011), and influence of smoke of fires on thunderstorm activity (Altaratz et al., 2010). Because the sensors of WWLLN detect the strokes, it is necessary to reconstruct the flashes. Cummins et al. (1998) described a process to identify strokes associated with a given flash by considering time and space criteria for the data from NLDN. They associate successive strokes in a flash when they are separated by less than 10 km in distance and less than 0.5 s in time, with a maximum duration of 1 s for the flash. In our case, we test several criteria because the accuracy and the efficiency of WWLLN are different compared to NLDN ones. Fig. 2 displays the ratio between the number of flashes and that of strokes for data from 2011, for two distinct time criteria of 0.5 and 1 s by considering variable distance criterion. It shows the curves for both values of dt are close, especially for values of distance lower than 20 km. On the other hand, the ratio changes more slowly with the distance, which means that the distance criterion can be taken beyond about 20 km without affecting much the number of flashes. Adopting the values 0.5 s and 20 km for the time and distance criteria respectively, an algorithm has been used to transform strokes data into flashes data for all nine years studied.

2.2. LIS data

LIS is an optical sensor of the scientific payload on the TRMM satellite (http://thunder.msfc.nasa.gov/lis/overview_lis_instrument.html), launched in December 1997 and ended in August 2014 (Christian et al., 1999; Boccippio et al., 2002; Chronis et al., 2008). It allows us to detect both IC and CG lightning flashes with an efficiency around 90%, but does not distinguish between them. It has a 350 km low orbit around the Earth (402 km after an orbit boost in August 2001), a 600 km × 600 km field-of-view, and an inclination of 35°, which allows the coverage of a region of the Earth between 38°N and 38°S (blue rectangle in Fig. 1). Due to the precession orbit, LIS is limited to roughly one overpass per day for any geographical location of the region covered. Its spatial resolution is between 3.9 and 5.4 km at nadir and limb, respectively (Christian et al., 1999). During a single orbit LIS can observe a given point on the Earth's surface for almost 90 s with a time resolution of 2 ms. During one year, the number of orbits comprised between 5704 and 5689, depending on whether it is a leap year or not. The data used in this study are available on the NASA website (http://thunder.msfc.nasa.gov/data) and correspond to lightning flashes reconstructed from the optical events detected by LIS, successively associated to make groups and flashes according to time and space criteria. Thus, the information given for a flash consists in the time of occurrence, the number of events, that of groups, the measured radiant energy and the estimated location.

3. Results

3.1. Overall lightning activity

WWLLN data are used for the analysis of the lightning activity in the area including the DRC territory. Table 1 displays several parameters related to the lightning activity in the area of the study and year by year. The first and second columns indicate the number of flashes detected by the WWLLN (N_W) and LIS (N_L). Both flash numbers are also displayed in Fig. 3 in order to visualize their respective evolution during the period of study and with comparable scales. A first look at the time series of N_W shows a first period of four years with a roughly constant amount of flashes except for 2007 that exhibits a specific increase. After 2008 N_W increases significantly and continuously to reach in 2013 about 3.5 times the value of 2005 (from 2,676,276 in 2005 to 9,181,456 in 2013). On the contrary, the number of flashes detected by LIS in the study area varies little and no tendency is

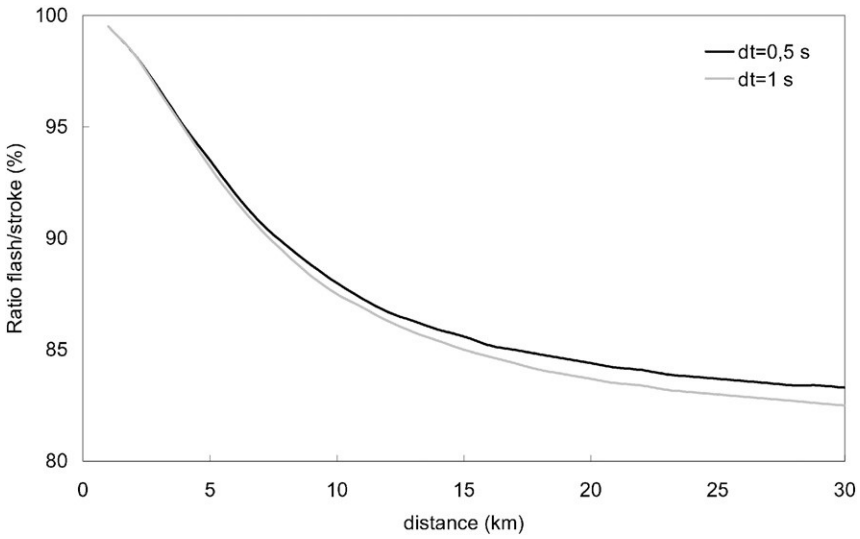

Fig. 2. Ratio (%) between the number of WWLLN flashes and that of strokes as a function of the distance criterion for two distinct time criteria.

Table 1
Annual count of lightning flashes detected by WWLLN (N_W) and by LIS (N_L), extrapolated total lightning flashes from LIS over the whole year and the whole study area (N_O). DE for the WWLLN relative to LIS for the study area and for the SWIO area (DE_B) from Bovalo et al. (2012). Maximum value of the number of stormy days (SD_{max}). Maximum value of the annual flash density from WWLLN (FD_{max}) and estimated by applying the DE factor (FD'_{max}). Average multiplicity M_m and proportion of flashes which produced only one stroke (M = 1).

	N_W	N_L	N_O	DE (%)	DE_B (%)	SD_{max} (day)	FD_{max} ($km^{-2}\,yr^{-1}$)	FD'_{max} ($km^{-2}\,yr^{-1}$)	M_m (str/fl)	M = 1 (%)
2005	2,676,276	190,308	153,761,877	1.74	2.00	114	2.70	155.17	1.071	93.73
2006	2,516,580	188,449	152,259,873	1.65	3.40	154	1.90	115.15	1.127	88.99
2007	3,602,064	182,653	147,568,838	2.44	5.00	131	2.66	109.02	1.111	90.64
2008	2,467,176	183,466	148,233,792	1.66	4.70	130	1.91	115.06	1.095	91.94
2009	3,446,317	195,316	157,808,157	2.18	6.60	143	3.93	180.28	1.116	90.32
2010	3,643,387	188,984	152,692,134	2.39	8.30	157	4.41	184.52	1.142	88.43
2011	4,701,732	192,007	155,134,607	3.03	8.50	167	4.63	152.81	1.185	85.37
2012	6,550,235	182,560	147,501,778	4.44	–	167	8.22	185.14	1.219	82.98
2013	9,181,456	192,443	155,486,879	5.90	–	189	12.86	217.97	1.278	79.62

observed during the period. Indeed, the minimum is 182,560 in 2012 while the maximum is 195,316 in 2009 (Table 1). N_L varies weakly during the whole nine-year period. Since the LIS detection ability did not change during the period, we can estimate that the lightning activity did not change significantly. The increase of the number of flashes detected by the WWLLN is mainly due to an improvement of DE during the same period. Several reasons can be evoked for such improvement: more stations were operated and the processing algorithm was more efficient (Rodger et al., 2008). Thus, a first step is to find a method to determine the relative detection efficiency of WWLLN in the study area since that of LIS is estimated for any region of the world (Boccippio et al., 2002).

3.2. Detection efficiency

For a same flash, WWLLN and LIS can give different locations since they do not measure the same physical parameters: WWLLN detects the stroke at the ground and LIS detects the cloud top illumination. Furthermore they differently associate the events relative to their number, timing and location. This aspect has to be kept in mind when a comparison is made between both data collections. Another difference between both databases is the time of coverage for a given region: WWLLN has a continuous coverage everywhere in the study domain while LIS covers a given point of this domain for about 90 s.

The surface swept by the LIS sensor after recovery of different orbits corresponds to the latitude band of 38°S to 38°N (Fig. 1). In this band, the elementary area is dS:

$$dS = R_T\, d\lambda R_T \cos\lambda\, d\varphi$$

where λ is the latitude, φ is the longitude and R_T is the Earth radius at the equator (R_T = 6378 km).

By integrating on the latitude band:

$$S_A = R_T^2 \int\int \cos\lambda\, d\lambda\, d\varphi = R_{T^2} \int \left(\int_{-38^\circ}^{38^\circ} \cos\lambda\, d\lambda \right) d\varphi$$

$$S_A = 4\pi {R_T}^2 \times 0.6157.$$

During a leap year (31,622,400 s), the satellite TRMM covers 5704 orbits. Thus, the average duration of one orbit is 31,622,400/5704 = 5543.89 s.

During one orbit, the area covered at the ground will be S_O = L × 600 km. L is the length of one orbit at the Earth surface: L = 2π R_T = 2π × 6378 = 40,074 km. S_O = 40,074 × 600 = 24,044,400 km^2.

Then, we define a surface coefficient: $\alpha_S = \frac{S_O}{S_A} = \frac{24{,}044{,}400}{4\pi R_T^2 \times 0.6157} = 0.07639$.

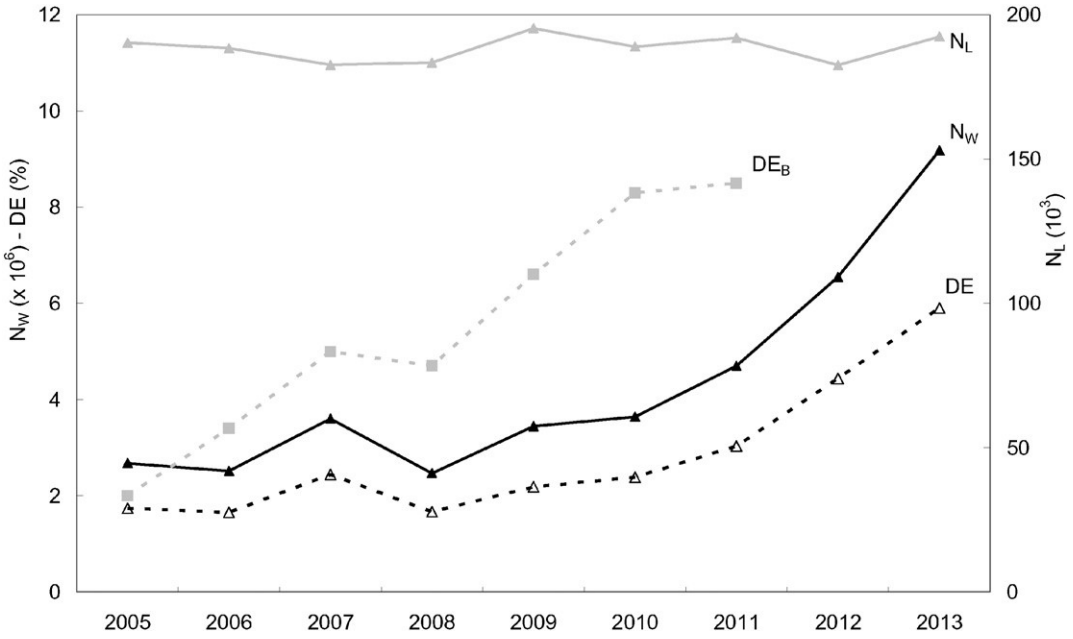

Fig. 3. Annual number of flashes detected by the WWLLN (N_W) and that detected by LIS (N_L), and estimated DE for WWLLN data relative to LIS data (DE) and that from Bovalo et al. (2012) (DE_B) for SWIO.

During one orbit, i.e. 5543.89 s, the surface covered is therefore 7.64% of the surface S_A. Furthermore, the satellite covers each point of this surface during only 90 s over the total 5543.89 s of the orbit. A time coefficient α_t has to be considered to estimate the proportion of the lightning activity that can be detected by LIS.

$$\alpha_t = \frac{90}{5544} = 0.0162$$

Thus, LIS sees each point of the surface covered during one orbit for 1.62% of the orbit duration. To summarize, during one orbit, LIS observes 7.64% (α_s) of the whole surface covered by the satellite during its successive passes and each surface point is observed during 1.62% (α_t) of the orbit duration. Consequently, the product $\alpha_s \times \alpha_t$ provides the time proportion during which a point is observed by LIS for the whole coverage of the band S_A:

$$\alpha = \alpha_s \times \alpha_t = 0.0764 \times 0.0162 = 0.00124 \text{ i.e.} 0.124\%.$$

This coefficient is applicable for any point of S_A and therefore for any point of the study area. We consider that statistically, according to the number of orbits described during one year, the sampling made by LIS is representative of the whole lightning activity for any region of the study area. Then we apply α to recover the total number of flashes N_O produced within the area from the number of flashes detected by LIS N_L:

$$N_L = \alpha N_O, \quad \text{therefore} \quad N_O = N_L/\alpha.$$

In order to evaluate DE for WWLLN relative to LIS, we take into account this coefficient α by dividing the number N_W of lightning flashes detected by WWLLN by the number of flashes N_O:

$$DE = \frac{N_W}{N_O} = \frac{N_W}{N_L} 0.00124.$$

The calculation of DE for each of the years 2005–2013 is included in Table 1 and compared with the detection efficiency DE_B found by Bovalo et al. (2012), for the South Western Indian Ocean (SWIO). The parameter DE increases year after year, except between 2005 and 2006, and between 2007 and 2009 since it markedly increases in 2007 and then decreases in 2008. From 1.65% in 2006 it increases to 5.90% in 2013. This evolution is roughly in agreement with the results of Bovalo et al. (2012) for the SWIO with DE_B that increases from 2.0 in 2005 to 8.5 in 2011. However, the increase is larger for DE_B compare to DE over the common period 2005–2011 since from close values around 2 for both parameters in 2005, DE is about doubled while DE_B is multiplied by 4 in 2011. The increase for 2007 is more pronounced for DE than for DE_B. The global increase of DE for WWLLN relative to LIS can be explained by an evolution of the network, or by the number of stations or by improving the algorithm of treatment used. According to Fig. 1, it is difficult to consider the number of stations to explain the difference between DE and DE_B because the new stations installed during the period 2005–2011 (La Réunion, Hermanus…) can improve the detection in both areas since they are at roughly equivalent distance. Furthermore a new station was installed close to DRC in 2010 in Nigeria (Fig. 1). The effect of a new station depends on the time of the year it was installed and it can be more visible during the year after its installation. Thus that installed in Nigeria will be more efficient for the flash amount in 2011, what is clearly shown in Table 1 since DE is 2.39 in 2010 and 3.03 in 2011. We have also to consider the different nature of the domains of both studies, mainly over the ocean for SWIO and over land for Congo Basin. The WWLLN may be more efficient to detect flashes over the ocean because the peak currents for CG flashes are generally larger and therefore easier to detect remotely (Seity et al., 2001). The study by DeMaria et al. (2012) devoted to investigate the relationships between the changes in the intensity of tropical cyclones and their lightning activity over two ocean areas during the period 2005–2010, also shows an increasing DE of the WWLLN. However for both areas, the increase was faster than that estimated in the present study above land area. Indeed, their total lightning DE was only about 1%–3% in 2005 according the area, and increased to about 20% by 2010 for both areas.

3.3. Annual lightning activity

Fig. 4 displays the annual evolution of the proportion of the flashes monthly detected by the WWLLN over the area. The histogram displays the proportion of the monthly activity averaged over the 9-year period. Two curves display the extreme values of this proportion within a 95% confidence interval in order to show the variability over the whole period. The average value smoothes the fluctuations from year to year and the dispersion around this average is included between 12% and 25% in relative values. For each year the same cycle is observed. Thus, a minimum of lightning activity is clearly identified during the months of June, July and August with a proportion of lightning activity around 4%. The maximum activity is over a period centered around December–January and of variable duration according to the year considered. According to the average monthly activity in Fig. 4, the period of the maximum lasts about six months from October to March.

According to Fig. 3, the number of flashes detected by the WWLLN significantly increases in 2007 and continuously from 2009. We compared the monthly flash number, month by month, between 2007 and 2006 on one hand, and between 2007 and 2008 on the other hand. In the present case, the irregularity of the flash number for a same month, from one year to another, does not allow to bring out the main reason of the increase of the number of flashes for 2007. Several reasons can explain this irregularity, as for example the natural variability of the storm activity or the breakdowns of some stations. On the same way, the same reasons do not allow to locate in time an improvement in DE at this scale of the month between 2009 and 2013.

Fig. 5a displays the distribution of the flashes detected in 2013 versus the multiplicity and Fig. 5b displays the evolution of the mean multiplicity M_m and that of the proportion of flashes with a multiplicity equal to one, i.e. the proportion of flashes with only one stroke detected. First of all, we can note the multiplicity is low, between 1.078 in 2005 and 1.278 in 2013. It is much lower than the multiplicity usually found for regional networks since it is close to 2 for the −CG flashes and a little higher than 1 for +CG flashes, like in the US with the NLDN (Orville and Huffines, 2001), or like in other regions of the world (Seity et al., 2001; Soriano et al., 2005). Secondly, the mean multiplicity increases when more flashes are detected, i.e. when DE increases as indicated in Fig. 5b. Indeed, except for 2007, the increase of M_m is consistent with the increase of DE shown in Table 1, while the proportion of flashes with $M = 1$ obviously decreases. Thus, the increase of DE leads to detect more flashes, as seen above, and more secondary strokes.

3.4. Diurnal evolution of the lightning activity

Fig. 6 displays the diurnal evolution of the lightning activity over the whole area, in terms of proportion hour by hour. The average proportion is represented by histograms while the variability over the whole period is plotted with two curves that display the minimum and maximum values within 95% confidence intervals. The dashed line displays the standard deviation. The proportion indicated at a given time corresponds to the flashes produced during one hour after this time. The evolution obtained is typical of the daily evolution for a land area as it is shown for example in Collier et al. (2006) for a part of southern Africa including most of the considered domain in the present study, in Liu and Zipser (2008) for tropical land regions around the world thanks to LIS data, or also in Proestakis et al. (2016) for midlatitude land area covered by ZEUS network. Thus, the minimum proportion is between 0600 and 0800 UTC (0700 and 0900 Local Time) and the

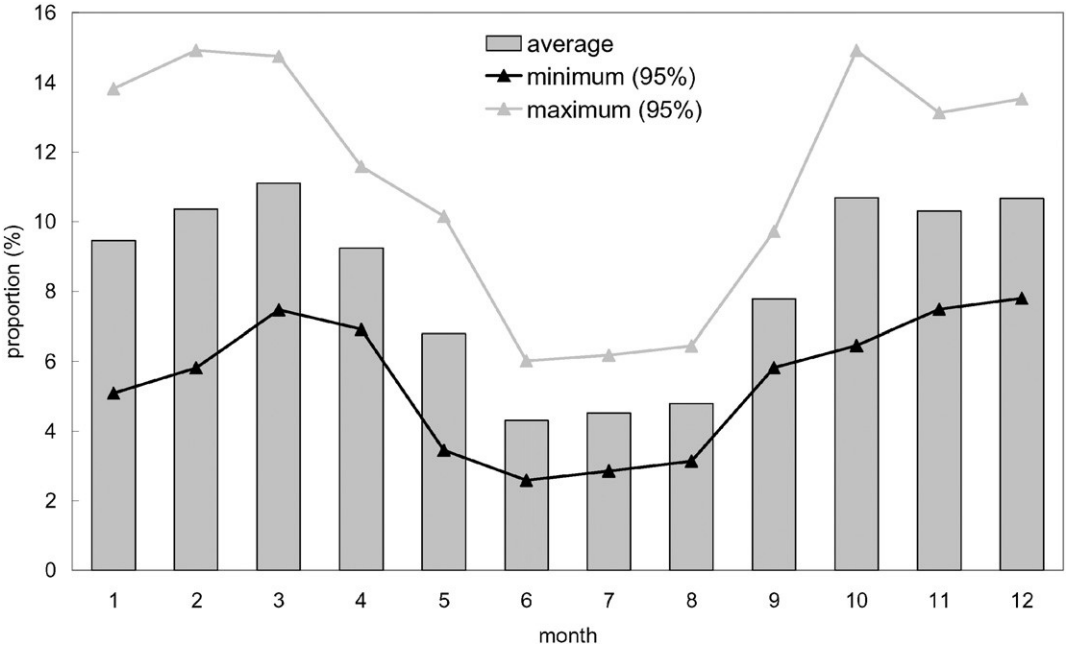

Fig. 4. Annual evolution of the monthly proportion of WWLLN flashes (%) averaged over the 9-year period (histogram), with indication of the 95% confidence interval (upper limit in grey and lower limit in black).

maximum is between 1600 and 1700 UTC (1700 and 1800 Local Time). However, the maximum can be earlier for some years, between 1400 and 1700 UTC. The ratio between the maximum and the minimum seems lower in the present study compared to most studies cited earlier, which can be due to long lifetime convective systems (Mesoscale Convective Systems) that can be active early in the day and that have a strong contribution to the rainfall in the Congo Basin (Mohr et al., 1999).

According to Fig. 6, the variability of the proportion is large during two periods of the day, around 0100 and 1400 UTC, and it is small during two other periods, around 0700 and 1900 UTC. Thus, the variability exhibits a 12-hour cycle, as indicated by the dashed line of the standard deviation (2 SD). It means the storm activity is more variable from one year to another around 0100 and 1400 UTC. The diurnal evolution can be different from one region to another as described in Venugopal et al. (2016). For example, for the area of the present study they show that the local maximum can be observed after 1500 UTC till 0600 UTC.

3.5. Lightning flash density

3.5.1. Overview

The lightning flash density has been calculated for each year with a resolution of and it has been expressed in flash per km^2 and per year (fl km^{-2} yr^{-1}). Fig. 7 displays the distribution of this density over the whole study area and for each year. As seen previously, the DE markedly changes during the period of study and consequently the flash density too. The scale is different for each graph corresponding to a year of the period and it is adapted to the range of the values to represent. The same trend is observed for each year: a sharp maximum of density is observed in a same and restricted region in the eastern DRC, around 28°E of longitude and around 1°S–2°S of latitude. The distribution of the density within this region will be analysed in detail further. However, it can be already noted that the yearly maximum value is always observed in this region of about 3° in latitude and 2° in longitude. The contrast of the density in this region with the rest of the area is variable from one year to another. Thus, the sharpness of this region in the distribution is stronger at the end of the period. Indeed, another region of large lightning density is visible in Fig. 7a–d from 2005 to 2008 in the center of DRC but for the following years (Fig. 7e–i) the lightning density in this large region is lower compared to the main maximum. The lightning density can be locally large some years, as for example along the coastline of Congo and Gabon in 2007.

Table 1 displays the maximum value of the lightning density FD_{max} from 2005 to 2013. First of all, the maximum density strongly increases from 2008 to 2013 whereas it oscillates between 1.9 and 2.7 fl km^{-2} yr^{-1} from 2005 to 2008. The largest value is found in 2013 with 12.86 fl km^{-2} yr^{-1}. Obviously, FD_{max} exhibits the same evolution as DE and N_W, the detection efficiency and the flashes detected by the WWLLN, respectively. Thus, the value of the maximum flash density is roughly multiplied by 6 over the whole period, while the flash number was only multiplied by a little less than 4. The value of the maximum density has to be put into perspective insofar it is very local at the scale of the study area. The maximum density of the total lightning FD'_{max} can be estimated by taking into account DE for the WWLLN calculated from LIS:

$$FD'_{max} = \frac{FD_{max}}{DE} \times 100.$$

Table 1 gives this estimation for the maximum density FD'_{max} for each year, and it ranges from 109.02 to 217.97 fl km^{-2} yr^{-1} at this 0.1° × 0.1° resolution. Of course these large values correspond to the total lightning activity as it would be seen by LIS with a full and continuous coverage.

Fig. 8a–b displays the distribution of the mean values of the lightning flash density from WWLLN data for two distinct periods, 2005–2008 (Fig. 8a) and 2009–2013 (Fig. 8b). As already noted from Fig. 7, the contrast between the sharp maximum located in the eastern DRC and the rest of the area is much more pronounced during the second period. Thus the wide region with relatively large values within the Congo Basin is much more visible during the first period. The largest value in the main maximum in the eastern DRC goes from 1.5 to 6.5 fl km^{-2} yr^{-1} from a period to another, while it goes from about 1 to 2 fl km^{-2} yr^{-1} in the Congo Basin. In order to verify if the difference observed between both periods is due to natural effects, the lightning activity observed from LIS is analysed in the same way. Thus, Fig. 8c–d displays the mean lightning flash density from LIS data for the same periods 2005–

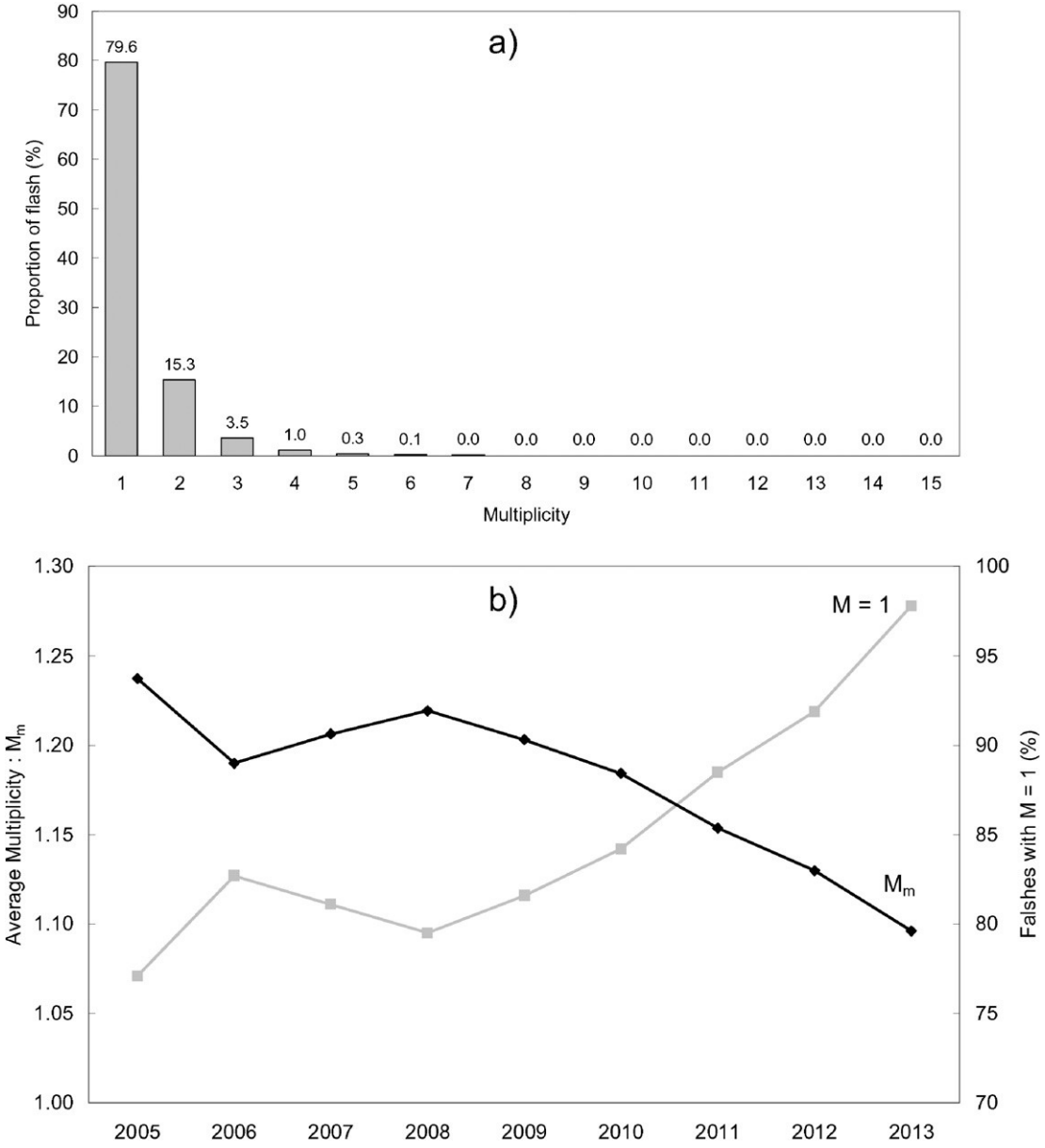

Fig. 5. a) Distribution of the WWLLN flashes versus multiplicity in 2013. b) Mean multiplicity M_m and proportion of WWLLN flashes with a multiplicity equal to 1 from 2005 to 2013.

2008 and 2009–2013. The difference of contrast observed from WWLLN data for both periods is not visible any more since both distributions are very close in terms of values and contrast. Indeed, both scales are identical and the distribution of the lightning density is really close for both graphs. Consequently, the difference observed from WWLLN data for both periods is probably due to an evolution of DE within the studied region.

Fig. 8e–f allows us to compare the lightning density pattern from WWLLN and that from LIS observations, for the whole period. Despite much stronger values for lightning flash density deduced from WWLLN data, the overall distribution exhibits the same characteristics: a sharp maximum in eastern DRC, a large region with moderate values of the density in the Congo Basin, some scattered and small regions with slightly larger densities as along the border between Gabon and Congo or the south-western DRC. Since the lightning density is averaged over the whole 9-year period, the values are lower than in the previous figure relative the last years of the period. The maximum density for the WWLLN is 4.07 $km^{-2}\ yr^{-1}$ in average over the whole period while for LIS it is 0.22 $km^{-2}\ yr^{-1}$. This difference is consistent with the ratio between the numbers of flashes detected by both systems N_W and N_L which is about 20 according to Table 1. In conclusion, the good agreement between the two distributions validates the representativeness of the observations by the WWLLN in terms of distribution.

3.5.2. Lightning density and number of stormy days

The previous figures show the flashes are not at all uniformly distributed over the area. Indeed, the flash density ranges from close to zero in some parts of the area (western part, over the ocean, the south-eastern DRC…) to much higher values, up to more than 12 $km^{-2}\ yr^{-1}$, locally. In order to compare the activity in the different regions, the number of days concerned by storms is calculated with a same resolution of 0.1° × 0.1°. Fig. 9 displays the pattern of the lightning density (a) and of the number of days with storms (b) in 2013. In a given pixel, a day is considered as stormy if at least one flash is detected. First of all the number of days is maximum where the density of flash is maximum in the eastern DRC. That means the large densities of lightning flashes are mainly due to large numbers of days with storm. However, the larger values of flashes are more spread and the contrast with

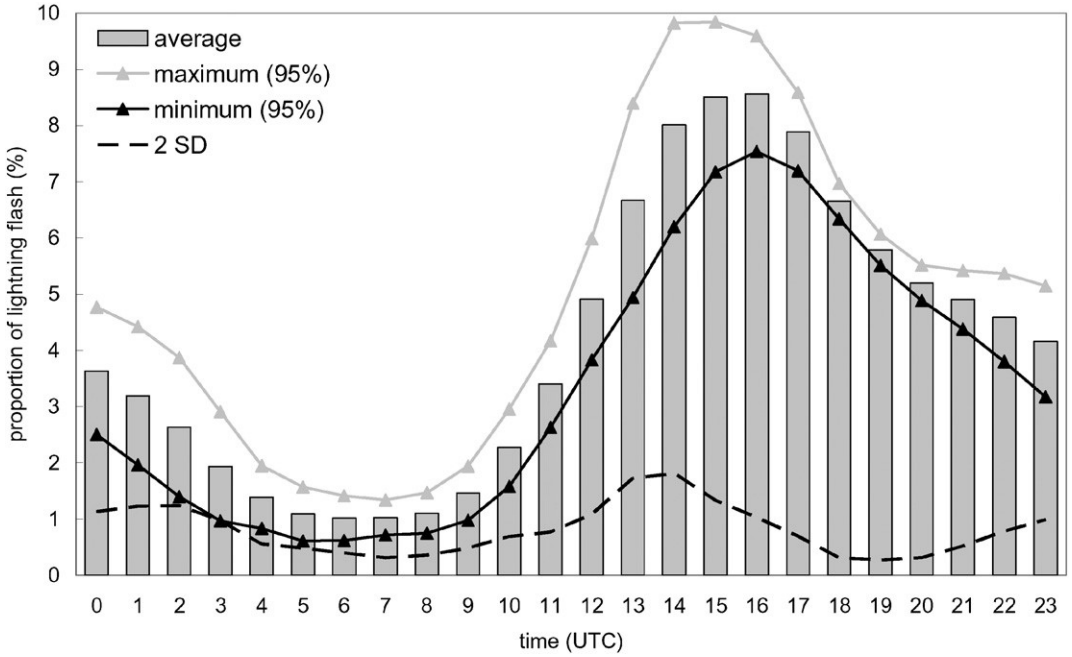

Fig. 6. Mean diurnal evolution of the lightning flash proportion (%) from WWLLN data over the 9-year period (histogram), with indication of the 95% confidence interval (upper limit in grey and lower limit in black), and standard deviation (dotted line).

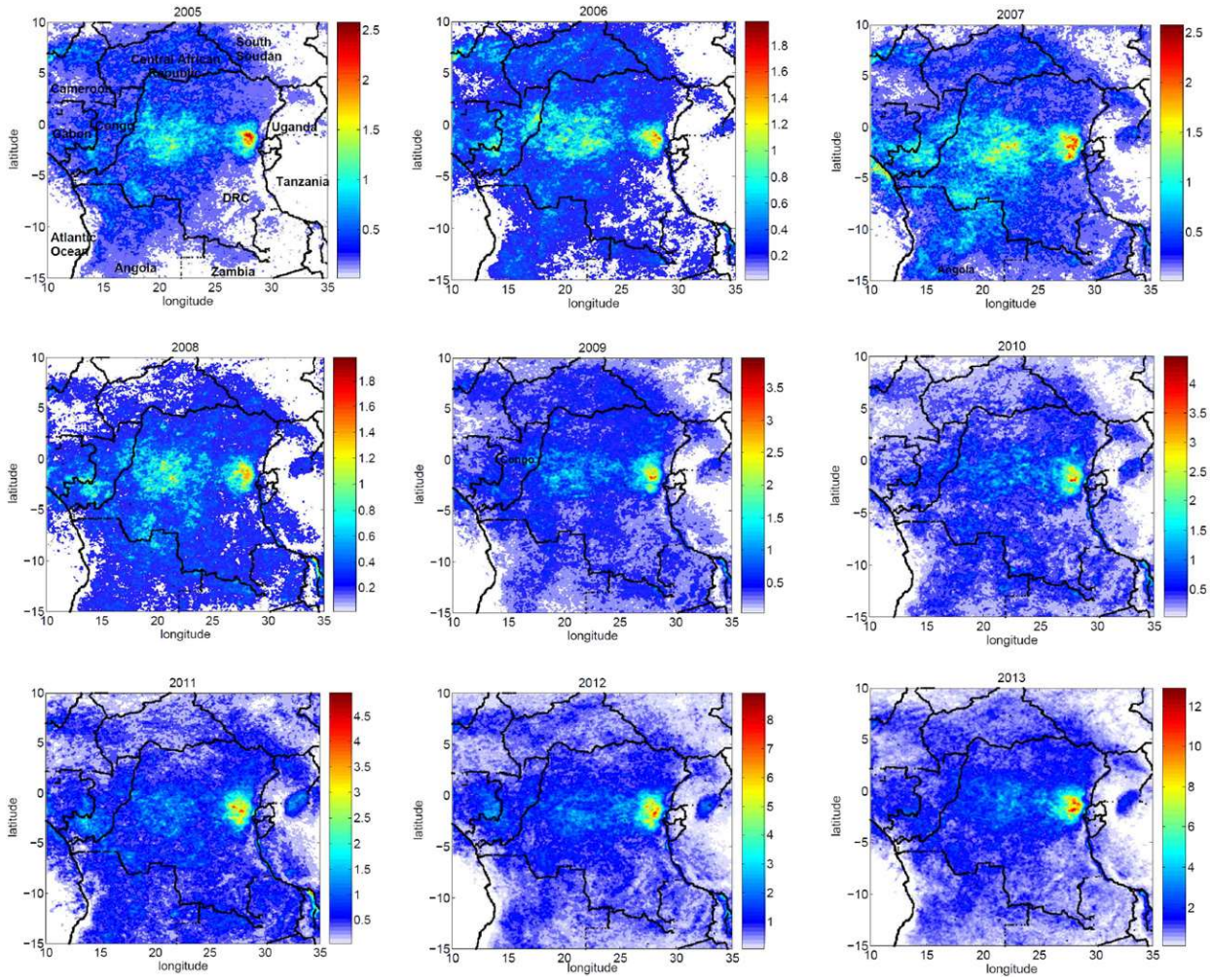

Fig. 7. WWLLN lightning flash density (fl km^{-2} yr^{-1}) in the study area (10°E–35°E; 15°S–10°N) from 2005 to 2013. Resolution is 0.1°× 0.1° and the scale is adapted for each graph with the maximum value.

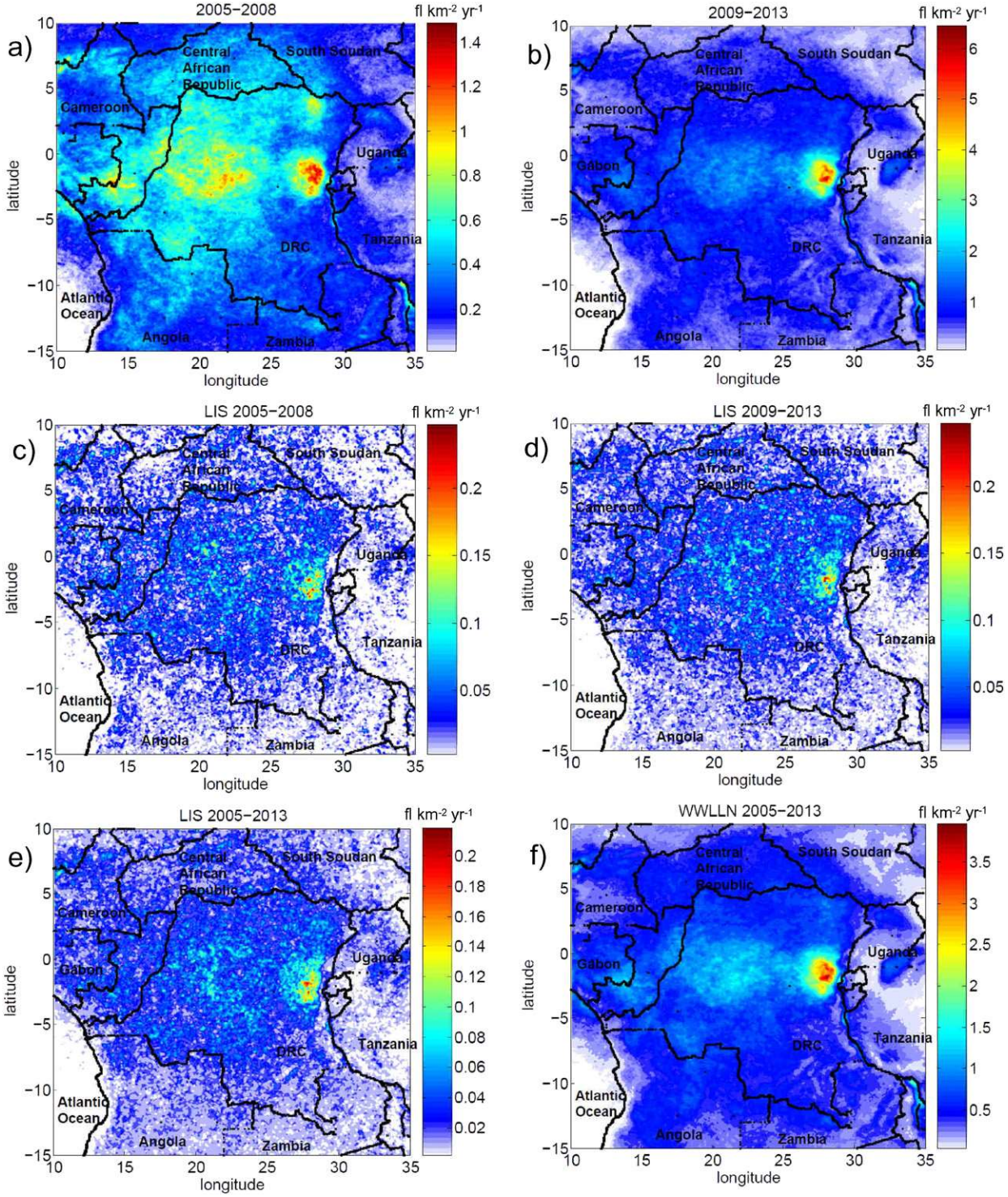

Fig. 8. WWLLN mean lightning flash density (fl km^{-2} yr^{-1}) for the periods 2005–2008 (a) and 2009–2013 (b). LIS mean lightning flash density (fl km^{-2} yr^{-1}) for the periods 2005–2008 (c) and 2009–2013 (d). Yearly lightning flash density (fl km^{-2} yr^{-1}) for the whole period 2005–2013 from LIS data (e) and from WWLLN data (f).

the rest of the area is stronger for the flash density. That means the maximum of flash density is not only due to a larger number of stormy days but also to more flashes during these stormy days. In order to compare the daily activity when storms occur, the average number of flashes per stormy day is calculated with the same space resolution and displayed in Fig. 9c. This parameter is less contrasted than the flash density or the storm day. It should be noted that this mean number of flashes per day is roughly larger in the regions of the maximum activity in terms of lightning density and number of days, especially in eastern DRC. In this region, the number of flash per day reaches around 8 fl day^{-1}, while it reaches around 5 fl day^{-1} in the central region of Congo Basin. The location of the largest values in the eastern DRC is consistent with Fig. 9a–b which shows a larger contrast for the lightning density in this region. It indicates that in this region the storms are either more active, or more stationary, or more numerous. Some very large values of the number of days are also locally observed in some regions of low flash densities and low number of days, i.e. regions of weak activity. It is for example the case along the west coastline along the

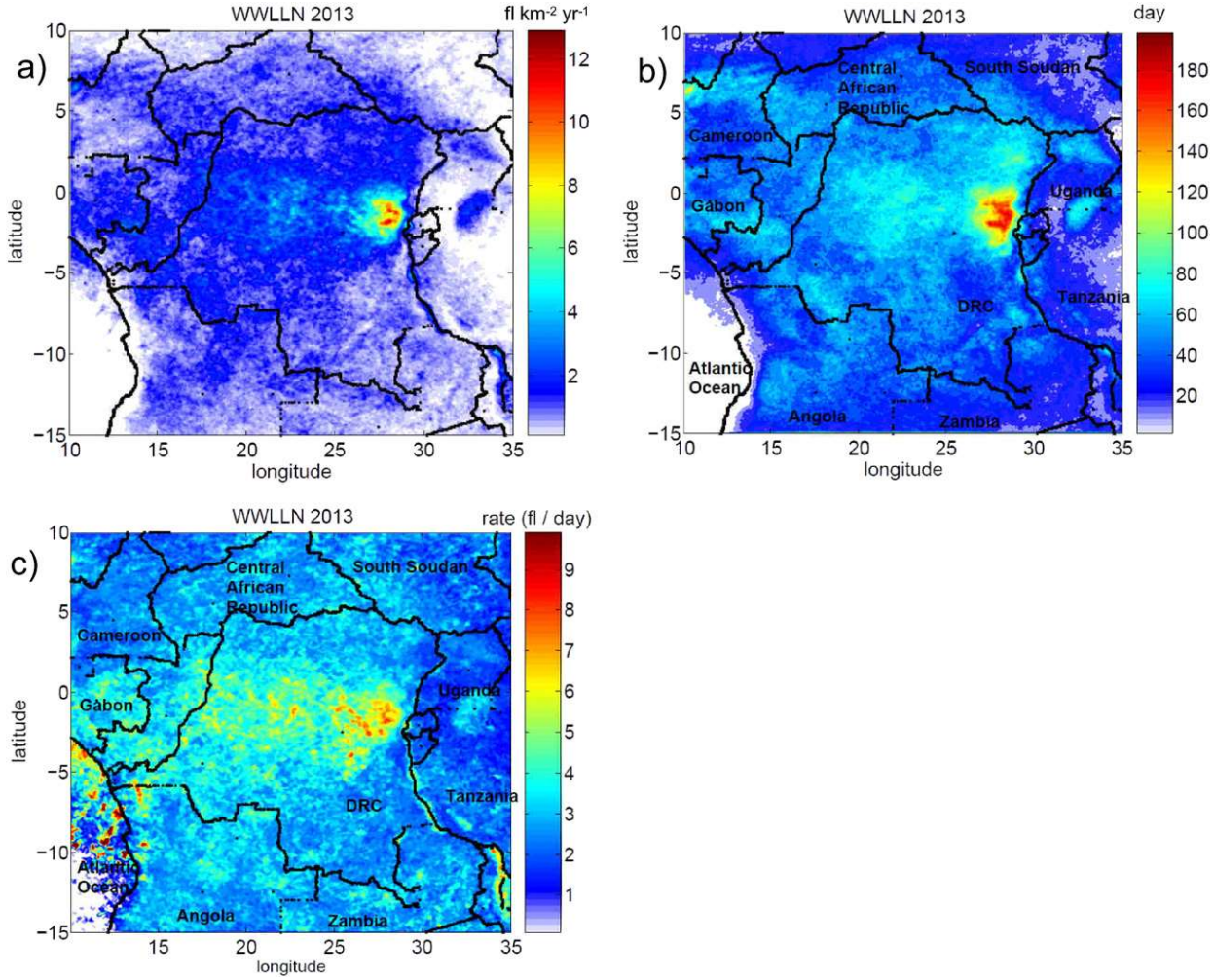

Fig. 9. Mean flash density (fl km^{-2} yr^{-1}) for 2013 (a) and number of stormy day for 2013 (b), from WWLLN data. (c) Flash number per stormy day (flash day^{-1}) for 2013.

Atlantic Ocean with values exceeding 10 fl day^{-1}. In these regions, storms are probably sparse but probably intense.

During the considered period, the maximum value of the number of stormy days increases from 114 days in 2005 to 189 days in 2013, while the maximum lightning density increases from 1.90 km^{-2} yr^{-1} in 2005 to 12.86 km^{-2} yr^{-1} in 2013 (Table 1). Comparatively, the increase of the lightning density is much more acute, which is due to the increase of DE for the WWLLN.

3.5.3. Seasonal evolution

Fig. 10 displays the distribution of lightning flash density in the whole area and in the region of the maximum for three distinct periods of 2013 characterized with specific lightning activity according to Section 3.3 and Fig. 4: a 6-month period of strong activity between October and March, a 3-month period of low activity between June and August, and a 3-month period including April, May and September. The scale of the lightning flash density is the same for each graph to compare the values of each period. These three periods represent 60.3%, 14.6%, and 25.1%, respectively, of the total amount of the flashes detected in 2013. These values are close to the average values for the whole 9-year period (2005–2013), 62.6%, 13.8% and 23.6%, respectively. The maximum values of the flash density for the three periods are 8.38 fl km^{-2}, 4.33 fl km^{-2}, and 3.67 fl km^{-2}, respectively. The ratios between these different maximum values are lower than those between the numbers of flashes because the maximum of density moves a little during the year, and therefore during a given period. This maximum is around 28°E in longitude but changes in latitude from 2°S for the October–March period to around 1°S for the other two periods. It favours local maxima development in this region as for example in Fig. 9a for 2013.

For the three periods, the region of the maximum is always very marked, but with more contrast for the period of strong activity (Fig. 10a–b). It is about of the same size, and located in the same region close and south of the equator. For the period of lower storm activity (Fig. 10c–d) most of the lightning activity is located north of the equator, except in the region of the maximum previously described and in a westwards region concerned by a secondary maximum. During this period, the lightning activity over the lakes is much lower, i.e. over the Lake Kivu (29°E; 2°S) and the Lake Victoria (33°E; 1°S). Generally, between the first period (Fig. 10a–b) and both others (Fig. 10c–f), the lightning density substantially decreases south of the equator. This is a characteristic of the seasonal storm activity that is everywhere observed in the world insofar more storms can develop when the sun elevation is higher.

3.5.4. Lightning density and surface characteristics

Fig. 11 shows a comparison of the mean lightning density for the whole period 2005–2013 with orography. The mean maximum value is about 4 fl km^{-2} in the eastern DRC which is roughly seven to eight times the mean values observed in most parts of the domain. Most of larger values of density are located south of the equator and it has to be noted that the lightning density is often enhanced over the main

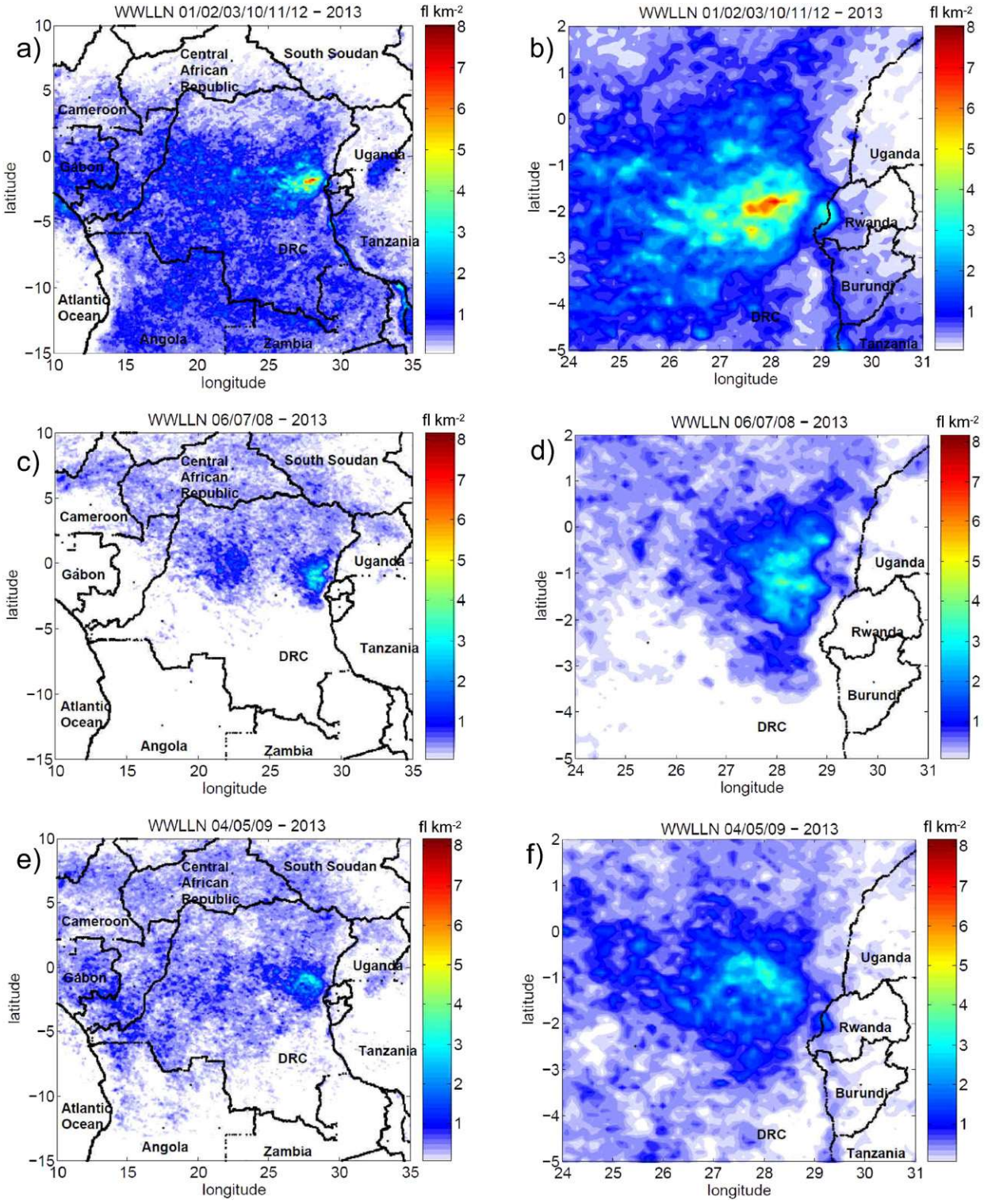

Fig. 10. Flash density (fl km^{-2}) from WWLLN data in the whole area (a, c, e) and in the maximum region (b, d, f) for three periods of 2013: (a) and (b) January–February–March–October–November–December, (c) and (d) June–July–August, (e) and (f) April–May–September.

lakes as Lake Victoria (33°E; 1°S) or Tanganyika Lake (34°E; 10°S). On the other hand, the lakes located further north apparently enhance less the lightning density, as for example Edouard Lake (29.67°E; 0.67°S) and Albert Lake (30.67°E; 1.33°N). The large region of secondary maximum of lightning density observed south to the equator and west of the sharp maximum, corresponds to forest areas which are characterized by altitudes below 1000 m westward. Small areas of larger densities are also observed in the western part of the area, especially over the Congo–Cameroon border (14°E; 2.5°S) and over the coastline of Gabon (11°E; 3.5°S).

The lightning density in the region of the main and sharp maximum is displayed in detail in Fig. 12a–d, for several years (2005, 2007, 2009 and 2013). The lightning density is averaged over the 9-year period to be representative of the whole period of study in terms of location

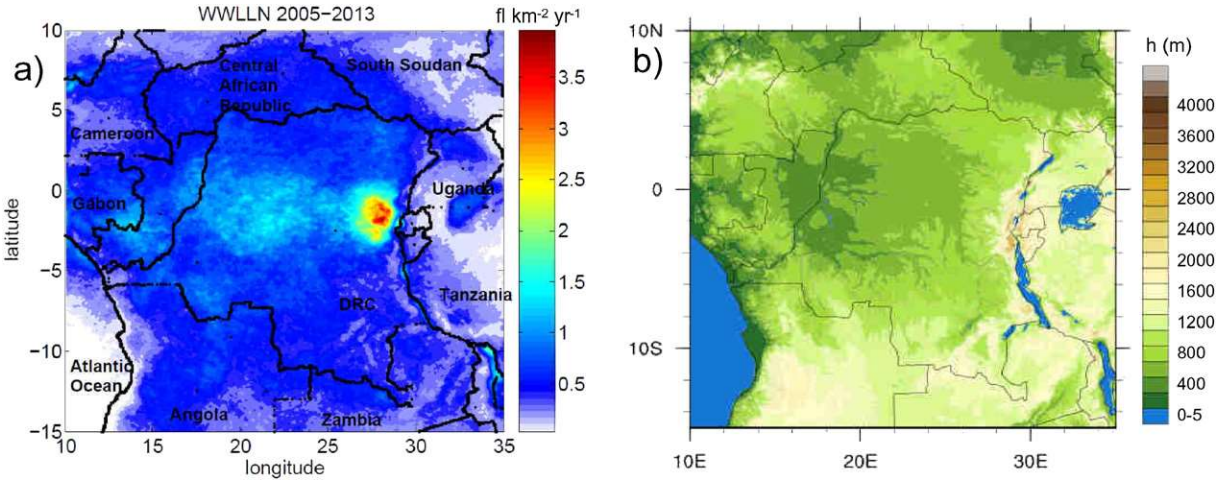

Fig. 11. a) Mean flash density (fl km^{-2} yr^{-1}) from WWLLN data in the whole area for the period 2005–2013. (b) Orography (m) in the same area.

and displayed in Fig. 12e. The orography of the region is displayed in Fig. 12f. The scale of lightning density is adapted to each graph and ranges between the minimum and the maximum value found in the area. Most of lakes exhibit a large lightning density as Lake Kivu (29.1°E; 2°S) and northern part of Tanganyika Lake (29.5°E; 3.5°S). As previously mentioned, the lightning density is lower for Edouard Lake and the southern part of Albert Lake. Above and surrounding the highest mountains of the region at more than 4000 m, especially on the border between DRC and Uganda (29.9°E; 0.4°N), the lightning density is lower.

The region with large values has about the same shape and size every year as indicated in Fig. 12a–d for different years and in Fig. 12e for the average over the period 2005–2013. It has an extension of about 300 km north–south and 200 km east–west and seems to exhibit two cores of larger values separated of about 75 km, one close to 1°S of latitude and the other close to 2°S. The maximum value can be located in one or the other core depending on the year. It is about 4 fl km^{-2} yr^{-1} and located in the southern core in Fig. 12e displaying the averaged density, at about 28.1°E of longitude and 1.8°S of latitude. The shape of the distribution of the mean density is similar to that of 2013, which reveals a stronger contribution of this year in the mean distribution. This region of large values is located westward of a south–north oriented mountain range characterized by summits at more than 2500 m close to Lake Kivu. Since the highest mountains exceeding 3000 m are located at about 28.5°E the presence of the mountains (white dashed line in Fig. 12e) can be a good candidate to explain the triggering of the convection and the large densities of lightning observed. Furthermore the orientation of the mountain range corresponds very well to that of the lines of constant density. The presence of lakes at the same latitude, Lake Kivu at small scale and Lake Victoria at large scale, can also provide moisture to help the thundercloud development.

4. Discussion and summary

The lightning activity issued from the WWLLN during a period of nine years has been analysed for an area of Central Africa including DRC, small surrounding countries and parts of others. This area corresponds to longitudes between 10°E and 35°E, latitudes between 15°S and 10°N, i.e. about 2750 km × 2750 km, and covers different types of relief between the sea level in the western part and mountain ranges exceeding 3000 m for some or 4000 m for others, in the eastern part. The detection system used in the WWLLN records a proportion of strokes produced by lightning flashes and a first step consisted in gathering strokes issued from a same flash according to time and space criteria. Tests on several values of these criteria between two successive strokes of a same flash leads to validate 0.5 s for the maximum time difference and 20 km for the distance. The distance criterion is larger than those usually found in the literature for regional detection networks, as for example 10 km proposed by Cummins et al. (1998) for the US NLDN, and Mäkelä et al. (2010) for the ALDIS network in northern Europe. This distance criterion usually corresponds to the maximum error of location of a stroke (Rivas and De Pablo, 2002) but for the present long range detection network WWLLN the error of location is obviously larger than 10 km. For the time criterion, it is of the same order than that for regional networks, usually fixed at 0.5 s between two successive strokes (Cummins et al., 1998), the baseline of the network has no influence on this parameter.

The criteria here considered for gathering strokes have been applied for each year of the studied period in order to focus on the number of flashes. Several parameters in relation with the flashes provided by the WWLLN change over the 9-year considered period, especially after 2008. For example the number of flashes is around 2,500,000 in the first four years and increases regularly from 2009 to reach 9,181,456 in 2013. The proportion of flashes with only one stroke decreases from about 90% during the first years to 80% in 2013, while the average multiplicity is around 1.1 at the beginning of the period and close to 1.3 at the end. The evolution of all these parameters is interpreted in terms of DE improvement by comparing with data provided by LIS during the same period over the same area. Indeed, the total number of flashes detected by this space sensor is almost constant year after year. The sample can be considered large enough since the yearly flash number from LIS is around 188,000. Its variation does not exceed more than 4% of this value. The total amount of flashes that LIS could detect by continuous observation of the study area is estimated from a simple space and time integration of data acquired by the orbiting sensor. It is estimated that the sensor detects only 0.124% of the total lightning flashes. The detection efficiency of the WWLLN relative to LIS evolves from ~2% during the first four years to ~6% in 2013. The trend is the same as in other parts of the world. By comparing with ocean regions, it is lower and it increases less rapidly. For example in SWIO, Bovalo et al. (2012) found 8.5% for 2011 while the present study provides a value close to 3%. Likewise, DeMaria et al. (2012) showed the WWLLN DE over two ocean basins increased faster during the period 2005–2010, from about 1% to 20% for East Pacific and from 3% to 20% for Atlantic. Rudlosky and Shea (2013) analyzed also the detection efficiency over a large area of western hemisphere during the period 2009–2012. They found the smallest values over land increasing from 4% to 6.4% during the period, large values over ocean increasing from 12.3% to 17.3%, with the largest values over north hemisphere, 10.7% in 2012, while it is 4.9% over south hemisphere. The present study gives 4.44% in 2012 for a land area mainly located

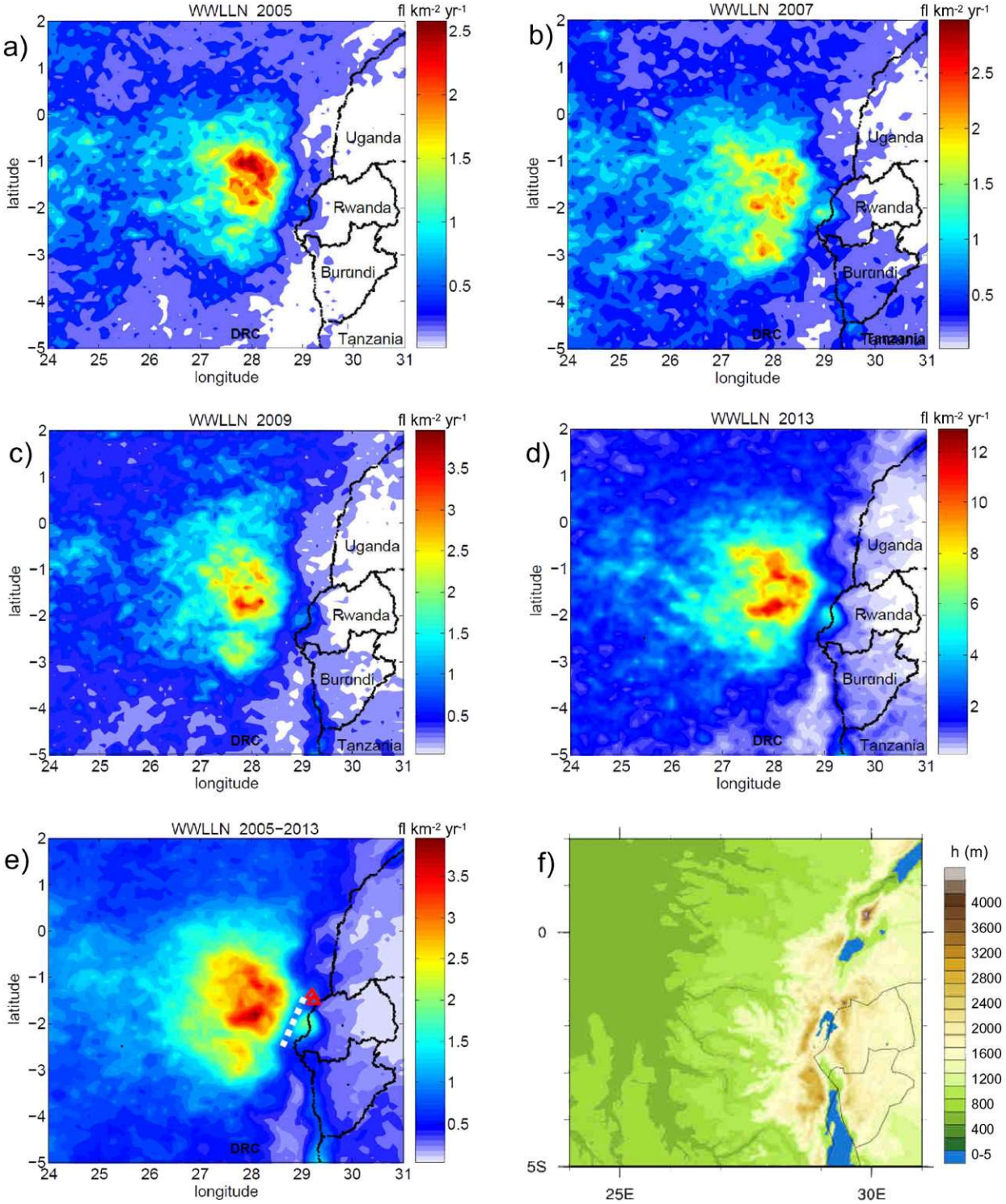

Fig. 12. Flash density (fl km^{-2} yr^{-1}) from WWLLN data in the maximum region for (a) 2005, (b) 2007, (c) 2009, (d) 2013, (e) the period 2005–2013. In e) the dashed line represents a mountain range west of Lake Kivu and red triangles two active volcanoes in the region. (f) Orography (m) in the same region.

in south hemisphere which is consistent with other observations. It is to be noted that DE is 44% higher in 2007 compared with previous or next year. Other studies confirm this tendency as Bovalo et al. (2012) and Rodger et al. (2008) who found an increase of 47% and of about 63%, respectively for the whole Earth because of the use of a new algorithm. However, the increase of DE is not continuous over the whole period, even at the scale of the year since it decreases for example from 2005 to 2006, or from 2007 to 2008. We can think that at the beginning of the period with a lower number of stations, the effect of a fault in a station may be stronger.

The annual cycle of lightning activity exhibits a period of high activity between October and March, during which about 10% of the total lightning flashes are produced each month, and a period of low activity from June to August with about 4.5% of the total flashes

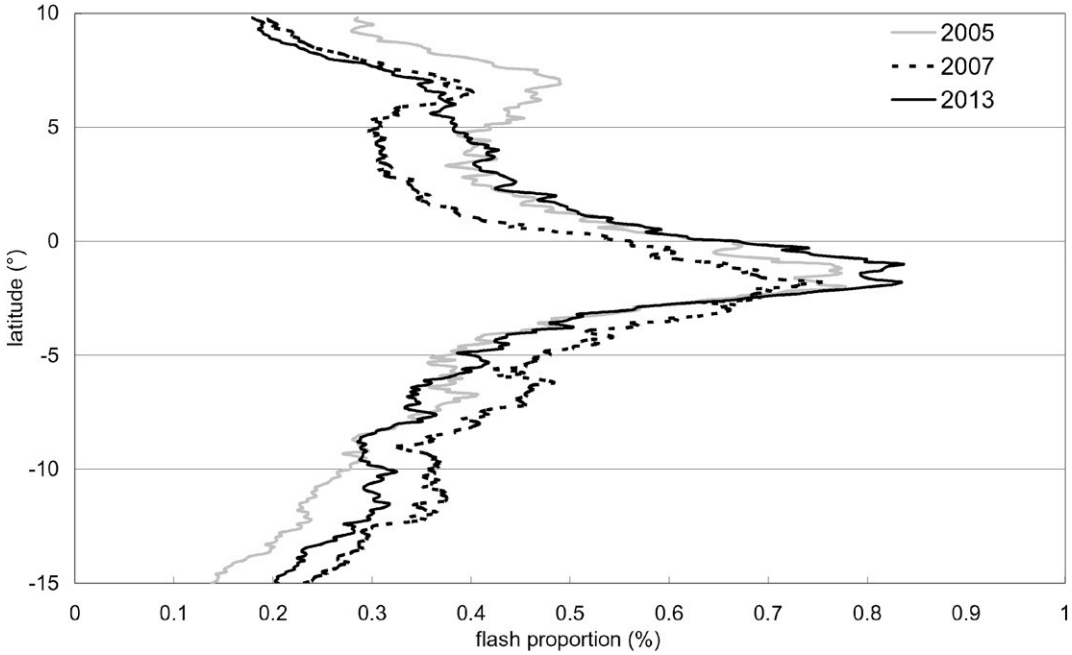

Fig. 13. Zonal distribution of the flashes (%) from WWLLN data, at a resolution of 0.1° for 2005, 2007 and 2013 in the whole area.

produced each month. Then, the lightning activity seems to follow the sun displacement above the study area since a proportion of 66.67% is located in the southern hemisphere. However, the distribution of the flashes is not symmetrical on both sides of the equator as indicated by different plots of the lightning density, while the yearly distribution of the sunshine is. The larger values of the density are mainly located south of the equator. If we compare the number of flashes on both sides of the equator up to 10 degrees latitude, 56.45% are located in the southern hemisphere, in average over the 9-year period. Fig. 13 displays the zonal distribution of flashes detected by WWLLN within the whole study area, in 2005, 2007 and 2013. This distribution confirms the dissymmetry with respect to the equator since its maximum is clearly localized in the southern hemisphere between 2°S and 1°S depending on the year. All yearly distributions present a similar global shape. This dissymmetry to the southern hemisphere over Africa was also observed for the highly reflective cloud from satellite observation by Waliser and Gautier (1993). By using this parameter for the ITCZ location they concluded its mean location was in the southern hemisphere for a slightly longer duration and at larger latitudes. Furthermore, they noted the ITCZ has a broader range over continent, especially for Africa. Likewise, Žagar et al. (2011) found the same dissymmetry for the zonal distribution of the precipitation over the African continent by using data from ERA Interim reanalyses. Thus, in their figure 4e displaying the meridional profiles of precipitation for different durations and over the whole continent, the annual profile exhibits a main maximum at a latitude of about 2–3°S and a secondary maximum at about 6–7°N, which strongly looks like the profiles in the present Fig. 13. They found also that over the tropical continents, the ITCZ is different whether it is determined from winds or precipitation criteria.

According to Nicholson (2009) and others, the ITCZ location strongly varies longitudinally over Africa and its mean location is more northward in western Africa, especially in January and its range is very broad along the year in eastern Africa, between 10°S in January and close to 15°N in August. Over the western region of the study area, the ITCZ varies a lot with latitude in January. The seasonal lightning density distributions confirm the observation from Christian et al. (2003) insofar the maximum density shifts northwards across the equator from December till June–August period according to the general ITCZ migration and associated forcing parameters as wind and convergence. As explained in Collier and Hughes (2011), the lightning activity does not exactly reflect the ITCZ location in Africa, since it depends on the underlying terrain and humidity of air.

The density of the lightning flashes can reach large values, even when DE is only 2% at the beginning of the period. We have to keep in mind that DE is calculated in reference to LIS that detects the whole lightning activity although WWLLN detects mainly the CG flashes. Furthermore, the lightning activity is very strong in this region of the world (Albrecht et al., 2011; Christian et al., 2013; Cecil et al., 2014). The maximum of the lightning activity is located in eastern DRC in a region along and part of a mountain range at altitudes that can exceed 3000 m, regardless of the reference year and the period of the year. In 2013, this maximum in terms of lightning flash density and number of stormy days reaches 12.86 fl km^{-2} and 189 days, respectively. Furthermore, the number of flashes per stormy day is located in the same region, which means the thunderstorms are there, more numerous, more intense, more stationary, or all three at once. The lightning density values are not representative and directly comparable to those from other regions of the Earth covered by regional lightning detection systems as for example the NLDN in US (Orville and Huffines, 2001) because the DE is low. The annual maximum value is systematically located in the eastern DRC, in the same area noted by many authors for the maximum over the whole Earth, as Christian et al. (2003) who falsely attributed it to Rwanda, Cecil et al. (2014), and Albrecht et al. (2011). By applying the DE issued from comparison with LIS data, the local maximum value of the total lightning flashes FD'_{max} is estimated for each year in the present study and reported in Table 1. The mean value is found equal to 157.23 fl km^{-2} yr^{-1}, which is quite comparable to the value 160 fl km^{-2} yr^{-1} reported by Albrecht et al. (2011). Because the resolution in the present study is 0.1° × 0.1° we find higher values than Christian et al. (2013) who reported 82.7 fl km^{-2} yr^{-1} from LIS at a resolution of 0.25° × 0.25°. Nevertheless, we find also the maximum is well located in the east part of Lake Kivu.

The main maximum of the lightning density found in the eastern region of the study area confirms the ITCZ location does not explain alone the lightning activity. This maximum is present along the year and it can be due to a combination of easterly humid air lifted by the relief located west of Lake Kivu. This observation clearly illustrates the observation made by Collier and Hughes (2011) reported above. According to a simulation of the climatology in the Basin of Lake

Victoria by Anyah et al. (2006), the prevailing easterly trades can transport moisture at large-scale and significantly enhance precipitation over the lake. As explained in Ba and Nicholson (1998) who studied the convective activity over the lakes in eastern Africa, convective precipitation over Lake Victoria is maximum early in the morning. In the present case, humidity may be transported from the Lake Victoria 500 km apart or from Indian Ocean more eastward. Indeed, according to the global lightning climatology, few lightning flashes are reported between the Indian Ocean and this maximum location (Christian et al., 2003). The presence of the mountain range as illustrated in Fig. 12e–f is a key element for the development of the storms likely to produce strong lightning density. Such situation is commonly observed close to Lake Maracaibo in Zulia state in Venezuela, in which Munoz et al. (2016) shows the role of the complex topography and the Maracaibo Basin Nocturnal Low Level Jet in lightning enhancement. Pujol et al. (2005, 2011) described and quantified the microphysical processes involved in the triggering and development of convective precipitation due to orographic effects, in presence of a lake. They noted the lake can act as a secondary moisture source which can favour local convection, and mountainous slopes favour updraughts which permits a downwind extension of the convective system by ejection of precipitating particles according to the fountain particles concept. Finally, by using observations and computation, they highlighted characteristics of the microphysics favourable to electric charging mechanisms in a configuration comparable to that of the local maximum observed in the present study.

The secondary maximum in Congo Basin that is broader might benefit favourable conditions for thunderstorm development as moist air due to local evaporation or advection from Guinea Gulf combined with lifting associated with the ITCZ from November till March since it is more pronounced during this period, especially for the first years. However, although less accurate, it is also present during the period June–August, and is therefore associated with local conditions. Since the orography is relatively smooth in this area, the conditions favourable for thunderstorm development would be mainly due to unstable humid air.

Acknowledgments

The authors thank the World Wide Lightning Location Network (http://wwlln.net/) for providing the lightning location data used in this study. They are grateful to US National Aeronautics and Space Administration (NASA) and Global Hydrology Resource Center (GHRC) for LIS data available on their website. JK is grateful to the French “Ministère des Affaires Etrangères”, to the French Embassy in DRC, especially Patrick Demougin, for supporting his stay in France and “Groupe International de Recherche en Géophysique Europe/Afrique” (GIRGEA) for cooperation organization, especially Christine Amory. JK thanks Professor Albert Kasadi from University of Kinshasa for his support, help and discussions all along the preparation of his contribution to the study.

References

Abarca, S.F., Corbosiero, K.L., 2011. The World Wide Lightning Location Network and convective activity in tropical cyclones. Mon. Weather Rev. 139, 175–191.

Abarca, S.F., Corbosiero, K.L., Galarneau, T.J., 2010. An evaluation of the Worldwide Lightning Location Network (WWLLN) using the National Lightning Detection Network (NLDN) as ground truth. J. Geophys. Res. 115, D18206. http://dx.doi.org/10.1029/2009JD013411.

Abreu, D., Chandan, D., Holzworth, R.H., Strong, K., 2010. A performance assessment of the World Wide Lightning Location Network (WWLLN) via comparison with the Canadian Lightning Detection Network (CLDN). Atmos. Meas. Tech. 3.1143–3.1153 http://dx.doi.org/10.5194/amt-3-1143-2010.

Albrecht, R.I., Goodman, S.J., Petersen, W.A., Buechler, D.E., Bruning, E.C., Blakeslee, R.J., Christian, H.J., 2011. The 13 years of TRMM lightning imaging sensor: from individual flash characteristics to decadal tendencies. Proceedings of the XIV International Conference on Atmospheric Electricity, 08–12 August 2011, Rio de Janeiro, Brazil.

Altaratz, O., Koren, I., Yair, Y., Price, C., 2010. Lightning response to smoke from Amazonian fires. Geophys. Res. Lett. 37, L07801. http://dx.doi.org/10.1029/2010GL042679.

Antonescu, B., Burcea, S., 2010. A cloud-to-ground lightning climatology for Romania. Mon. Weather Rev. 138, 579–591. http://dx.doi.org/10.1175/2009MWR2975.1.

Anyah, R.O., Semazzi, F.H.M., Xie, L., 2006. Simulated physical mechanisms associated with climate variability over Lake Victoria Basin in East Africa. Mon. Weather Rev. 134, 3588–3609.

Ba, M.B., Nicholson, S.E., 1998. Analysis of convective activity and its relationship to the rainfall over the Rift Valley Lakes of east Africa during 1983–90 using the Meteosat infrared channel. J. Appl. Meteorol. 37, 1250–1264.

Boccippio, D.J., Koshak, W.J., Blakeslee, R.J., 2002. Performance assessment of the optical transient detector and lightning imaging sensor. Part I: predicted diurnal variability. J. Atmos. Ocean. Technol. 19, 1318–1332.

Bovalo, C., Barthe, C., Begue, N., 2012. A lightning climatology of the South-West Indian Ocean. Nat. Hazards Earth Syst. Sci. 12, 2659–2670. http://dx.doi.org/10.5194/nhess-12-2659-2012.

Bovalo, C., Barthe, C., Yu, N., Bègue, N., 2014. Lightning activity within tropical cyclones in the South West Indian Ocean. J. Geophys. Res. Atmos. 119, 8231–8244. http://dx.doi.org/10.1002/2014JD021651.

Burgesser, R.E., Nicora, M.G., Avila, E.E., 2012. Characterization of the lightning activity of “Relampago del Catatumbo”. J. Atmos. Sol. Terr. Phys. http://dx.doi.org/10.1016/j.jastp.2012.01.013.

Cecil, D., Buechler, D.E., Blakeslee, R.J., 2014. Gridded lightning climatology from TRMM-LIS and OTD: dataset description. Atmos. Res. 135, 404–414. http://dx.doi.org/10.1016/j.atmosres.2012.06.028.

Christian, H.J., Blakeslee, R.J., Boccippio, D.J., Boeck, W.L., Buechler, D.E., Driscoll, K.T., Goodman, S.J., Hall, J.M., Koshak, W.J., Mach, D.M., Stewart, M.F., 2003. Global frequency and distribution of lightning as observed from space by the Optical Transient Detector. J. Geophys. Res. 108 (D1), 4005. http://dx.doi.org/10.1029/2002JD002347.

Christian, H.J., Blakeslee, R.J., Goodman, S.J., Mach, D.A., Stewart, M.F., Buechler, D.E., Koshak, W.J., Hall, J.M., Boeck, W.L., Driscoll, K.T., Boccippio, D.J., 1999. The lightning imaging sensor. Proceedings of the 11th International Conference on Atmospheric Electricity. NASA, Huntsville, AL, pp. 746–749.

Chronis, T.G., Goodman, S.J., Cecil, D., Buechler, D., Robertson, F.J., Pittman, J., Blakeslee, R.J., 2008. Global lightning activity from the ENSO perspective. Geophys. Res. Lett. 35, L19804. http://dx.doi.org/10.1029/2008GL034321.

Collier, A.B., Hughes, A.R.W., 2011. Lightning and the African ITCZ. J. Atmos. Sol. Terr. Phys. 73.2392–73.2398 http://dx.doi.org/10.1016/j.jastp.2011.08.010.

Collier, A.B., Hughes, A.R.W., Lichtenberger, J., Steinbach, P., 2006. Seasonal and diurnal variation of lightning activity over southern Africa and correlation with European whistler observations. Ann. Geophys. 24, 529–542. http://dx.doi.org/10.5194/angeo-24-529-2006.

Cummins, K.L., Murphy, M.J., Bardo, E.A., Hiscox, W.L., Pyle, R.B., Pifer, A.E., NLDN'95, 1998. A combined TOA/MDF technology upgrade of the US National Lightning Detection Network. J. Geophys. Res. 103, 9,035–9,044.

DeMaria, M., DeMaria, R.T., Knaff, J.A., Molenar, D., 2012. Tropical cyclone lightning and rapid intensity change. Mon. Weather Rev. 140, 1828–1842. http://dx.doi.org/10.1175/MWR-D-11-00236.1.

Dowden, R.L., Brundell, J.B., Rodger, C.J., 2002. VLF lightning location by time of group arrival (TOGA) at multiple sites. J. Atmos. Sol. Terr. Phys. 64, 817–830.

Hodanish, S., Sharp, D., Collins, W., Paxton, C., Orville, R.E., 1997. A 10-yr monthly lightning climatology of Florida: 1986–95. Weather Forecast. 12, 439–448.

Jacobson, A.R., Holzworth, R., Harlin, J., Dowden, R., Lay, E., 2006. Performance assessment of the Worldwide Lightning Location Network (WWLLN) using the Los Alamos Sferic Array (LASA) array as ground truth. J. Atmos. Ocean. Technol. 23, 1082–1092.

Liu, C., Zipser, E., 2008. Diurnal cycles of precipitation, clouds, and lightning in the tropics from 9 years of TRMM observations. Geophys. Res. Lett. 35, L04819. http://dx.doi.org/10.1029/2007GL032437.

Mäkelä, A., Tuomi, T.J., Haapalainen, J., 2010. A decade of high-latitude lightning location: effects of the evolving location network in Finland. J. Geophys. Res. 115, D21124. http://dx.doi.org/10.1029/2009JD012183.

Mohr, K.I., Famiglietti, J.S., Zipser, E.J., 1999. The contribution to tropical rainfall with espect to convective system type, size and intensity estimated from 85-GHz ice-scattering signature. J. Appl. Meteorol. 38, 596–606.

Munoz, A.G., Daz-Lobaton, J., Chourio, X., Stock, M.J., 2016. Seasonal prediction of lightning activity in north western Venezuela: large-scale versus local drivers. Atmos. Res. 172, 147–162.

Nicholson, S.E., 2009. A revised picture of the structure of the ‘monsoon’ and land ITCZ over West Africa. Clim. Dyn. 32 (7–8), 1155–1171.

Orville, R.E., Huffines, G.R., 2001. Cloud-to-ground lightning in the United States: NLDN results in the first decade, 1989–98. Mon. Weather Rev. 129, 1179–1193.

Proestakis, E., Kazadzis, S., Lagouvardos, K., Kotroni, V., Kazantzidis, A., 2016. Lightning activity and aerosols in the Mediterranean region. Atmos. Res. 170, 66–75.

Pujol, O., Georgis, J., Chong, M., Roux, F., 2005. Dynamics and microphysics of orographic precipitation during MAP-IOP3. Q. J. R. Meteorol. Soc. 131, 2795–2819.

Pujol, O., Lascaux, F., Georgis, J.-F., 2011. Kinematics and microphysics of MAP-IOP3 event from radar observations and Meso-NH simulations. Atmos. Res. 101 (1–2), 124–142.

Rivas, L., De Pablo, F., 2002. Study of lightning event duration and flash rate in the Iberian Peninsula using cloud-to-ground lightning data. Atmos. Res. 61, 189–201.

Rodger, C.J., Brundell, J.B., Dowden, R.L., 2005. Location accuracy of long distance VLF lightning location network: post algorithm upgrade. Ann. Geophys. 23, 277–290.

Rodger, C.J., Brundell, J.B., Holzworth, R.H., Lay, E.H., 2008. Growing detection efficiency of the World Wide Lightning Location Network. Am. Inst. Phys. Conf. Proc., Coupling of Thunderstorms and Lightning Discharges to Near-Earth Space: Proceedings of the

Workshop, Corte (France), 23–27 June 2008. Vol. 1118, pp. 15–20. http://dx.doi.org/10.1063/1.3137706.
Rodger, C.J., Werner, S., Brundell, J.B., Lay, E.H., Thomson, N.R., Holzworth, R.H., Dowden, R.L., 2006. Detection efficiency of the VLF World-Wide Lightning Location Network (WWLLN): initial case study. Ann. Geophys. 24, 3197–3214.
Rudlosky, S.D., Shea, D.T., 2013. Evaluating WWLLN performance relative to TRMM/LIS. Geophys. Res. Lett. 40. http://dx.doi.org/10.1002/grl.50428.
Seity, Y., Soula, S., Sauvageot, H., 2001. Lightning and precipitation activities in coastal thunderstorms. J. Geophys. Res. 106 (D19), 22,801–22,816.
Soriano, L.R., De Pablo, F., Tomas, C., 2005. Ten-year study of cloud-to-ground lightning activity in the Iberian Peninsula. J. Atmos. Sol. Terr. Phys. 67, 1632–1639.
Soula, S., van der Velde, O.A., Montanya, J., Huet, P., Barthe, C., Bór, J., 2011. Gigantic jets produced by an isolated tropical thunderstorm near Réunion Island. J. Geophys. Res. 116, D19103. http://dx.doi.org/10.1029/2010JD015581.
Venugopal, V., Virts, K., Sukhatme, J., Wallace, J.M., Chattopadhyay, B., 2016. A comparison of the fine-scale structure of the diurnal cycle of tropical rain and lightning. Atmos. Res. 169, 515–522.
Waliser, D.E., Gautier, C., 1993. A satellite-derived climatology of the ITCZ. J. Clim. 6 (11), 2162–2174.
Williams, E., Stanfill, S., 2002. The physical origin of the land–ocean contrast in lightning activity. C.R. Phys. 3, 1277–1292. http://dx.doi.org/10.1016/S1631-0705(02)01407-X.
Žagar, N., Skok, G., Tribbia, J., 2011. Climatology of the ITCZ derived from ERA interim reanalyses. J. Geophys. Res. 116, D15103. http://dx.doi.org/10.1029/2011JD015695.